Optical Materials 45 (2015) 219–223

Contents lists available at ScienceDirect

Optical Materials

journal homepage: www.elsevier.com/locate/optmat

Photoluminescence properties of γ-$Ca_3(PO_4)_2$:Sm^{3+} prepared under high-pressure and high-temperature conditions

Weihong Xue [a,b,*], Shuangmeng Zhai [a], Shiqing Xu [c]

[a] Key Laboratory of High-Temperature and High-Pressure Study of the Earth's Interior, Institute of Geochemistry, Chinese Academy of Sciences, Guiyang 550002, China
[b] Key Laboratory of Orogenic Belts and Crustal Evolution, MOE; School of Earth and Space Sciences, Peking University, Beijing 100871, China
[c] College of Materials Science and Engineering, China Jiliang University, Hangzhou 310018, China

ARTICLE INFO

Article history:
Received 5 November 2014
Received in revised form 17 February 2015
Accepted 22 March 2015
Available online 7 April 2015

Keywords:
Photoluminescence
γ-$Ca_3(PO_4)_2$:Sm^{3+}
WLED
Concentration quenching

ABSTRACT

γ-$Ca_3(PO_4)_2$:Sm^{3+} samples were synthesized under high-pressure and high-temperature conditions. The samples were characterized by X-ray diffraction measurements. The excitation and emission spectra and fluorescence decay curves of synthesized samples were collected to study the photoluminescence properties. The excitation spectra of γ-$Ca_3(PO_4)_2$:Sm^{3+} exhibit a series of narrow peaks attributed to the typical f–f transition of Sm^{3+}. The emission spectra of γ-$Ca_3(PO_4)_2$:Sm^{3+} compose of four bands attributed to transitions from $^4G_{5/2}$ excited state to $^6H_{J/2}$ (J = 5, 7, 9 and 11) ground states of Sm^{3+}. The average decay lifetimes were obtained by fitting the decay curves for $^6H_{7/2}$ level of Sm^{3+} emission using a double exponential function. The photoluminescent spectra of γ-$Ca_3(PO_4)_2$:Sm^{3+} show that the samples belong to a red-emitting phosphor and can be pumped in the near ultraviolet light region, which can easily be applied for NUV LED chips and thus in WLEDs. There exists a concentration quenching of Sm^{3+} in γ-$Ca_3(PO_4)_2$:Sm^{3+} samples. The critical concentration of Sm^{3+} in γ-$Ca_3(PO_4)_2$ is about 1.0 mol%.

1. Introduction

Phosphates were regarded as important hosts for phosphor and luminescent materials, and many phosphates doped with different lanthanides were investigated [1–16]. Among those phosphates, β-tricalcium phosphate (β-TCP, β-$Ca_3(PO_4)_2$) is one of the important calcium phosphates. Previous study shows that β-TCP is not stable under high-pressure and high-temperature conditions. At 4 GPa and 950 °C, β-TCP transforms into γ-tricalcium phosphate (γ-TCP, γ-$Ca_3(PO_4)_2$) [17]. There is a significant difference in the crystal structures between β-TCP and γ-TCP. In β-TCP, five kinds of Ca exist complicatedly with coordinated number of 3, 6, 7, 8 and 8, respectively [18]. However, only two kinds of Ca exist with coordinated number of 10 and 12 in γ-TCP [19]. Due to the crystal structure, γ-TCP is regarded as an important host for rare earth elements (REE) [19]. Actually, REE-bearing γ-TCP was obtained in high-pressure and high-temperature experiments [20].

A series of trivalent REE cations have photoluminescence and have been widely used in cathodoluminescence, display phosphor screens, lasers, and lamps due to their f–f or d–f transitions [21–24]. It is interesting to investigate the luminescent properties of γ-TCP doped with REE. In our previous study, Eu^{3+}-doped γ-TCP was investigated [25]. As we known, trivalent samarium (Sm^{3+}) is another most important luminescence center. Sm^{3+} has a fundamental level $^6H_{5/2}$ and three main emitting levels $^4G_{5/2}$, $^4F_{3/2}$ and $^4G_{7/2}$, which gives visible reddish-orange emission and exhibits relatively high quantum efficiency forming a practical view point for lighting and displays [26,27]. Sm^{3+}-doped β-TCP was recently prepared and the luminescent properties were characterized [28]. In this study, Sm^{3+}-doped γ-TCP samples were first synthesized in high-pressure and high-temperature experiments and the luminescence properties of the samples were investigated.

2. Experimental

2.1. Sample preparation

The Sm^{3+}-doped γ-TCP samples were synthesized under high-pressure and high-temperature conditions by using the mixture of β-$Ca_3(PO_4)_2$ and Sm_2O_3 (99.99%) as starting material. The experimental procedure is similar to that described in our previous study [25]. The Sm^{3+} doping concentrations were 0.25%, 0.5%, 1.0%, 1.5% and 2.0% (in molar ratio), respectively. The experiments were carried out using a 1000-tonne Kawai-type apparatus (USSA-1000) installed at Institute for Study of the Earth's Interior, Okayama

* Corresponding author at: Institute of Geochemistry, Chinese Academy of Sciences, Guiyang, Guizhou 550002, China. Tel.: +86 851 5895692.
E-mail address: xueweihong@vip.gyig.ac.cn (W. Xue).

http://dx.doi.org/10.1016/j.optmat.2015.03.042
0925-3467/

University, Japan. An 18/11 sample assembly is adopted, as illustrated in Fig. 1. The thermal insulators were ZrO_2 tube and rods. The heater was graphite. Two platinum capsules enclosed different mixtures of Sm_2O_3 (99.99%) and β-TCP were put in one experiment. Between the graphite heater and Pt capsules, MgO sleeve was inserted. The temperature was monitored by a thin $W_{97}Re_3$/$W_{75}Re_{25}$ thermocouple whose junction was set at the center of the sample assembly. Quenched method was used to synthesize Sm^{3+}-doped γ-TCP samples. The experimental conditions were selected as 8 GPa and 1000 °C for 10 h based on the sample assembly and the phase relationship of $Ca_3(PO_4)_2$ [29]. After pressure was applied, temperature was raised. The samples were kept at desired pressure and temperature conditions for 10 h, and then they were quenched by turning off the electric power supply. Finally the samples were decomposed to the ambient pressure.

2.2. Characterization

The synthesized samples were ground into fine powder and checked by powder X-ray diffractometer (Rigaku's Smartlab) using rotating anode Cu Kα irradiation. The acceleration voltage and the current were 40 kV and 30 mA, respectively. The XRD patterns were collected in the 2θ range from 25° to 80° with step size of 0.01°. The photoluminescence excitation and emission spectra and fluorescence decay curves of the synthesized samples were recorded with a Jobin-Yvon FL3-211-P spectrofluorometer, using a 370-nm pulsed spectral-LED and Xe lamp as an excitation source for the samples.

3. Results and discussion

3.1. Powder X-ray diffraction

γ-TCP crystallizes in a rhombohedral structure with the space group R-3 m (No. 166) [19,30]. Phosphorus atom is tetrahedrally coordinated by oxygen atoms. Calcium atoms are located at two crystallographic sites of Ca(1) and Ca(2) with coordination numbers of 12 and 10, respectively. Along the *c* axis, the structure can be expressed by a translationally interconnected polyhedral sequence PO_4–$Ca(2)O_{10}$–$Ca(1)O_{12}$–$Ca(2)O_{10}$–PO_4. The powder XRD patterns of 0.25–2.0 mol% Sm^{3+}-doped γ-TCP samples are shown in Fig. 2. The XRD patterns of synthesized β-TCP and γ-TCP are also illustrated. The XRD results indicate that Sm^{3+}-doped γ-TCP samples show an identical structure with γ-TCP since all peaks can be indexed to the γ-$Ca_3(PO_4)_2$ phase according to PDF 32-176, and no obvious impurity phase was detected when Sm^{3+} ions were doped into the host lattice. The unit cell parameters of synthesized samples were listed in Table 1. With increasing of Sm concentration, the lattice parameters slightly increase. It is well-known that the radius of Sm^{3+} (0.96 Å) is similar to that of Ca^{2+} (1.00 Å). Therefore, the substitution of Ca^{2+} by Sm^{3+} is easy in γ-TCP. A substituted mechanism involving a vacancy at Ca sites, i.e., $2Sm^{3+} + \square = 3Ca^{2+}$, is responsible for the present study. Indeed, such substituted mechanism involving vacancy was confirmed in previous studies on other rare earth elements in apatites [31,32]. There are two kinds of Ca^{2+} in γ-TCP, but we cannot determine the occupancy of Sm^{3+} in γ-TCP. According to mass balance, CaO should appear in the sample. However, due to the relative low intensity of peaks and overlapping with those of γ-TCP, it is difficult to index peaks of CaO in XRD patterns.

3.2. Photoluminescence spectra

The luminescent properties of Sm^{3+} (0.25–2.0 mol%) doped γ-TCP samples were investigated at room temperature. Fig. 3 shows the excitation spectra (λ_{em} = 601 nm) of Sm^{3+}-doped γ-TCP samples with various concentrations. Sm^{3+}-doped γ-TCP samples exhibit a series of narrow peaks attributed to the typical f–f transition of Sm^{3+} ions. The results show the bands corresponding to transitions: $^6H_{5/2} \rightarrow (^4K, {}^4L)_{17/2}$ (340 nm), $^6H_{5/2} \rightarrow (^4D, {}^6P)_{15/2}$ (357 nm), $^6H_{5/2} \rightarrow {}^4L_{17/2}$ (370 nm), $^6H_{5/2} \rightarrow {}^4K_{11/2}$ (399 nm), $^6H_{5/2} \rightarrow {}^6P_{5/2} + {}^4M_{19/2}$ (413 nm), $^6H_{5/2} \rightarrow {}^4G_{9/2} + {}^4I_{15/2}$ (435 nm), and $^6H_{5/2} \rightarrow {}^4F_{5/2} + {}^4I_{13/2}$ (470 nm), respectively [13]. It is noted that the strongest excitation sharp line corresponding to the $^6H_{5/2} \rightarrow {}^4K_{11/2}$ transition of Sm^{3+} located at 399 nm, which indicates that the samples can be pumped in the NUV light region, and can easily be applied for NUV LED chips and thus in WLEDs [33].

The emission spectra (λ_{exc} = 399 nm) of Sm^{3+}-doped γ-TCP samples were illustrated in Fig. 4. There are four main sharp emission peaks at 563, 597, 646 and 704 nm, among which the most intense peaks are centered at 597 nm. The emissions are caused by the f–f forbidden transitions of the 4f electrons of Sm^{3+}, corresponding to

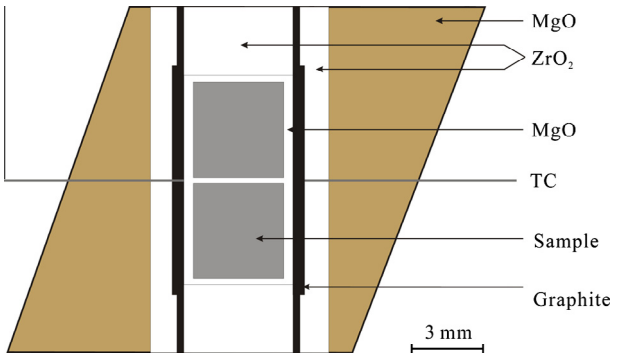

Fig. 1. Schematic drawing of the 18/11 sample assembly.

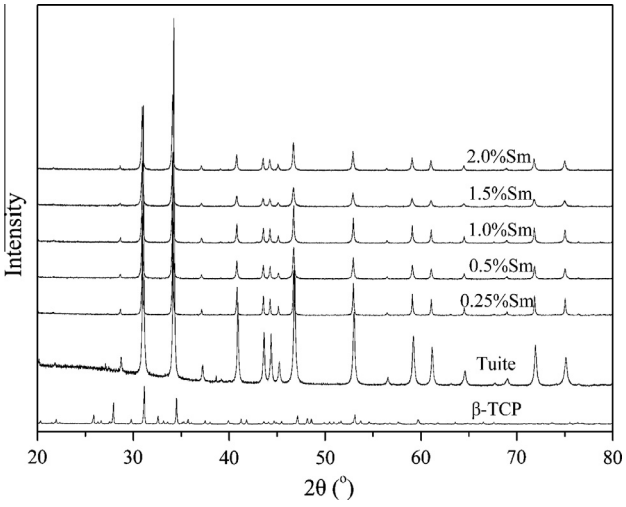

Fig. 2. X-ray diffraction patterns of β-TCP, γ-TCP and Sm^{3+} (0.25–2.0 mol%) doped γ-$Ca_3(PO_4)_2$ samples.

Table 1
Unit cell parameters, average life time (τ) and CIE of γ-$Ca_3(PO_4)_2$:Sm^{3+} samples.

Sm (mol%)	*a* (Å)	*c* (Å)	*V* (Å^3)	τ (ms)	*x*	*y*
0	5.2524(4)	18.681(3)	446.30(5)	–	–	–
0.25	5.2531(3)	18.688(2)	446.60(6)	0.61	0.55	0.45
0.5	5.2536(5)	18.690(2)	446.74(8)	0.62	0.57	0.43
1.0	5.2547(4)	18.694(2)	447.02(7)	1.50	0.58	0.42
1.5	5.2557(4)	18.698(2)	447.29(7)	0.86	0.58	0.42
2.0	5.2570(5)	18.703(3)	447.63(2)	0.80	0.58	0.42

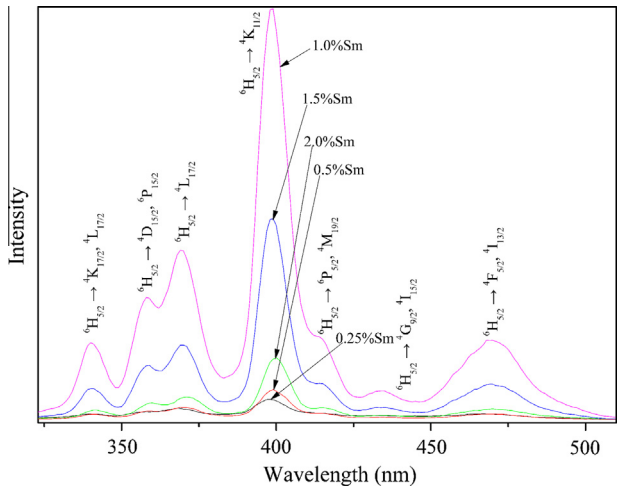

Fig. 3. The excitation spectra of Sm^{3+} (0.25–2.0 mol%) doped γ-$Ca_3(PO_4)_2$ samples.

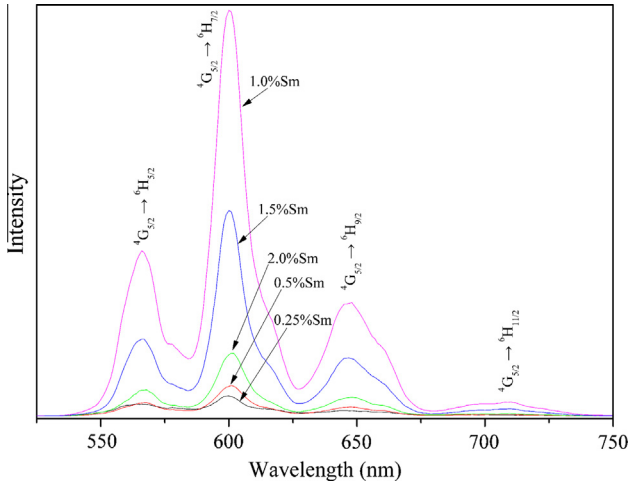

Fig. 4. The emission spectra of Sm^{3+} (0.25–2.0 mol%) doped γ-$Ca_3(PO_4)_2$ samples.

$^4G_{5/2} \rightarrow {}^6H_{5/2}$ (563 nm), $^4G_{5/2} \rightarrow {}^6H_{7/2}$ (597 nm), $^4G_{5/2} \rightarrow {}^6H_{9/2}$ (646 nm) and $^4G_{5/2} \rightarrow {}^6H_{11/2}$ (704 nm), respectively [13].

It is obviously observed that the intensity of peaks in excitation and emission spectra change with the concentration of Sm^{3+} while the peak locations remain practically unchanged. The excitation and emission intensity initially increases with the Sm^{3+} concentration increasing from 0.25 to 1.0 mol%, and then decreases as the Sm^{3+} concentration increases from 1.0 to 2.0 mol%, showing energy migration between Sm^{3+} at different sites in the lattice. The excitation band with the highest intensity was the 399 nm one, corresponding to the $^6H_{5/2} \rightarrow {}^4K_{11/2}$ transition for Sm^{3+}. And the emission band with the highest intensity was the 597 nm one, corresponding to the $^4G_{5/2} \rightarrow {}^6H_{7/2}$ transition for Sm^{3+}. Fig. 5 shows the relative intensity of excitation and emission bands with different concentration of Sm^{3+} ions. It should be pointed out that the intensity was normalized to highest intensity of each transition of Sm^{3+} ions. The relative intensity of each transition of Sm^{3+} ions shows similar trends for both excitation and emission bands. As the Sm^{3+} concentration increases, the excitation and emission intensities of each transition gradually increase and reach a maximum at 1.0 mol%. The concentration quenching happens since the intensity decreases when the concentration increases from 1.0 to 2.0 mol%.

The causes of concentration quenching may be attributed to the facts that the activated Sm^{3+} concentration is higher, the distance

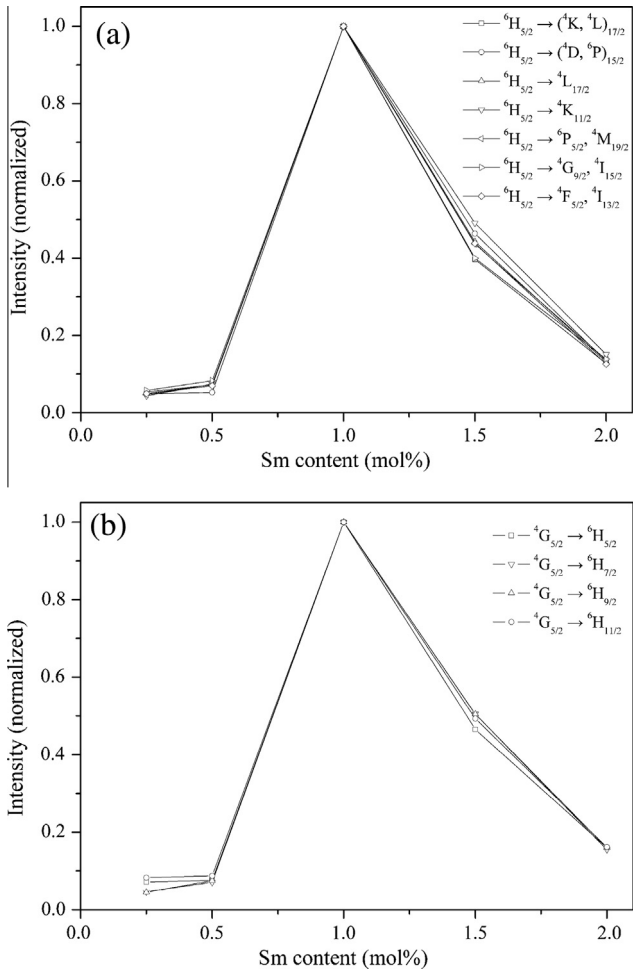

Fig. 5. Effect of Sm contents on the excitation (a) and emission (b) intensities of typical transitions of Sm^{3+} ions in γ-$Ca_3(PO_4)_2$ host.

between the ions is shorter, ionic bonding interaction enhances and the non-radiative energy transfer Sm ($^4G_{5/2}$) + Sm ($^6H_{5/2}$) → Sm ($^6F_{9/2}$) happens [22,24]. It is dependent on the critical distance R_c as the shortest average distance between the nearest activator Sm^{3+} ions at a critical concentration x_c. Previous study pointed out that if the activator is introduced solely on Z ion sites, the critical transfer distance R_c is approximately equal to twice the radius of a sphere with this volume, expressed as the following equation [34]:

$$R_c \approx 2\left(\frac{3\,V}{4\pi\, x_c N}\right)^{1/3}. \quad (1)$$

where V is the unit cell volume, x_c is critical concentration, and N is the number of Z cations in the unit cell. By using the available values of V, x_c and N (445.57 Å^3, 0.01 and 6, respectively), the critical distance is calculated to be about 24.21 Å.

In order to obtain additional information on the luminescence properties of Sm^{3+} ions in γ-$Ca_3(PO_4)_2$ host, the decay curves of the Sm^{3+} emission at 601 nm corresponding to the $^4G_{5/2} \rightarrow {}^6H_{7/2}$ emission line have been measured and given in Fig. 6. As shown in Fig. 6, the decay curves for $^6H_{7/2}$ level of Sm^{3+} emission can be well fitted into a double exponential function as follows:

$$I(t) = I_0 + A_1 \exp(-t/\tau_1) + A_2 \exp(-t/\tau_2). \quad (2)$$

where I and I_0 are the luminescence intensity at time t and 0, A_1 and A_2 are constants, t is the time, and τ_1 and τ_2 are the decay times for

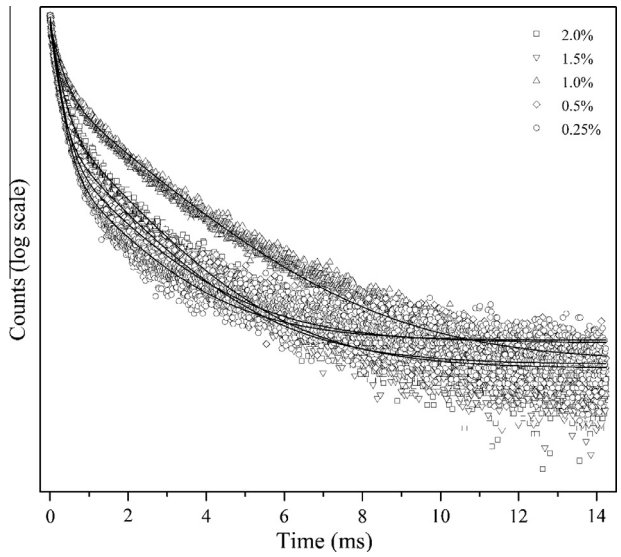

Fig. 6. Decay curves of the Sm^{3+} emission at 601 nm corresponding to the $^4G_{5/2} \rightarrow {}^6H_{7/2}$ emission line for Sm^{3+} (0.25–2.0 mol%) doped γ-$Ca_3(PO_4)_2$ samples. The solid curves represent fittings by using a double exponential function.

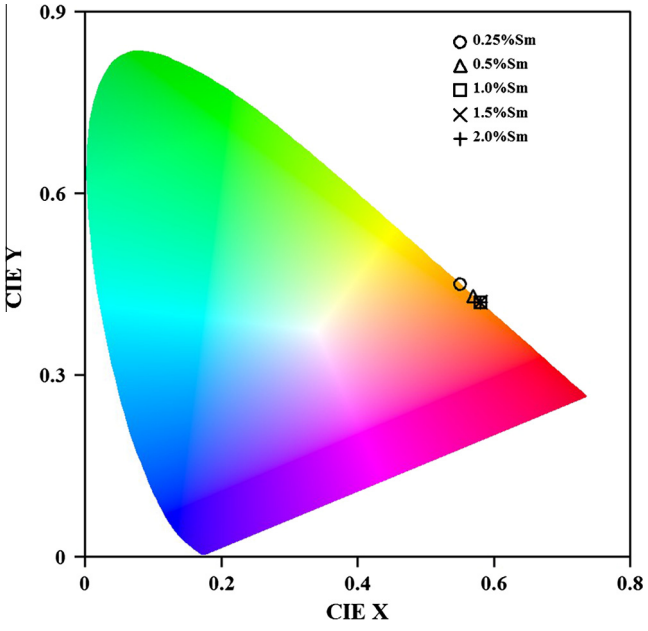

Fig. 7. CIE chromaticity coordinates of the Sm^{3+} (0.25–2.0 mol%) doped γ-$Ca_3(PO_4)_2$ samples.

the exponential components, respectively. Further, the average decay lifetimes (τ) can be calculated as follows:

$$\tau = (A_1\tau_1^2 + A_2\tau_2^2)/(A_1\tau_1 + A_2\tau_2). \quad (3)$$

The analysis yields the average decay lifetime as 0.61, 0.62, 1.50, 0.86, and 0.80 ms for the Sm concentration of 0.25, 0.5, 1.0, 1.5, and 2.0 mol%, respectively, as listed in Table 1. Obviously, an effect of Sm concentration on the decay lifetime of the samples exists. The 1.0 mol% Sm doped sample is with the longest decay lifetime.

Color is usually communicated on the basis of the color coordinates established by the Commission International de l'Eclairage (CIE) 1931, in a two-dimensional graphical representation of any color perceptible by the human eye on an x–y plot. The obtained results were shown in Table 1 and Fig. 7. The CIE of 0.25 and 0.5 mol% Sm^{3+}-doped γ-TCP are about $x = 0.55$, $y = 0.45$, and $x = 0.57$, $y = 0.43$, as an open circle and open triangle in Fig. 7, and the CIEs of other three samples are merged due to the same $x = 0.58$ and $y = 0.42$. The present results are slight different from that of Sm^{3+}-doped β-$Ca_3(PO_4)_2$ (0.615,0.385) [28], but close in proximity to the Nicha corporation-developed amber LED NSPAR70BS (0.575,0.425) and locates in the red[1] region (0.57,0.41). The CIE chromaticity coordinates of present samples hardly change with the doped Sm^{3+} concentrations. The result is easily comprehensible because the location of the luminescent emission dose not shift and the dominant emission does not change, as shown in Fig. 4. The results are consistent with previous studies [28,33].

4. Conclusions

Novel red phosphor γ-$Ca_3(PO_4)_2$:Sm^{3+} was synthesized at high-pressure and high-temperature conditions. The synthesized samples exhibited an intense emission at 597 nm. The relationship between the luminescent intensity and the concentration of activated ions Sm^{3+} shows that there is concentration quenching of Sm^{3+}-doped γ-$Ca_3(PO_4)_2$, and the critical concentration is 1.0 mol%. The CIE of Sm^{3+}-doped γ-$Ca_3(PO_4)_2$ show that they are suitable to near-UV LEDs as the red phosphors.

Acknowledgements

The authors thank G. Ye for the helps of photoluminescence measurements. We gratefully appreciate the support from the Institute for Study of the Earth's Interior, Okayama University, to carry out the high-pressure and high-temperature experiments and check the samples by powder X-ray diffractometer. This work was financially supported by the National Natural Science Foundation of China (Grant Nos. 41202020 and 41372040).

References

[1] J. Dexpert-Ghys, R. Mauricot, M.D. Faucher, J. Lumin. 69 (1996) 203.
[2] R. Reisfeld, M. Gaft, G. Boulon, C. Panczer, C.K. JØrgensen, J. Lumin. 69 (1996) 343.
[3] R. Ternane, M. Trabvelsi-Ayedi, N. Kbir-Ariguib, B. Piriou, J. Lumin. 81 (1999) 165.
[4] R. Ternane, G. Panczer, M.T. Cohen-Adad, C. Goutaudier, G. Boulon, N. Kbir-Ariguib, M. Trabelsi-Ayedi, Opt. Mater. 16 (2001) 291.
[5] R. El Ouenzerfi, C. Goutaudier, M.Th. Cohen-Adad, G. Panczer, G. Boulon, J. Lumin. 102–103 (2003) 426.
[6] N. Lakshminarasimhan, U.V. Varadaraju, J. Solid State Chem. 177 (2004) 3536.
[7] S.G.C. Vicente, M.A.M. Gamez, A.V. Kir'yanov, G.A. Kumar, Opt. Mater. 27 (2005) 1563.
[8] K. Madhukumar, H.K. Varma, M. Komath, T.S. Elias, V. Padmanabhan, C.M.K. Nair, Bull. Mater. Sci. 30 (2007) 527.
[9] I.M. Nagpure, S.J. Dhoble, Manoj Mohapatra, Vinay Kumar, Shreyas S. Pitale, O.M. Ntwaeaborwa, S.V. Godbole, H.C. Swart, J. Alloys Compd. 509 (2011) 2544.
[10] F. Chen, X. Yuan, F. Zhang, S. Wang, Opt. Mater. 37 (2014) 65.
[11] W. Geng, G. Zhu, Y. Shi, Y. Wang, J. Lumin. 155 (2014) 205.
[12] A. Lira, A. Speghini, E. Camarillo, M. Bettinelli, U. Caldiño, Opt. Mater. 38 (2014) 188.
[13] F. Yang, Y. Liu, X. Tian, G. Dong, Q. Yu, J. Solid State Chem. 225 (2015) 19.
[14] Y. Liu, A. Lan, Y. Jin, G. Chen, X. Zhang, Opt. Mater. 40 (2015) 122.
[15] Q. Xu, J. Sun, D. Cui, Q. Di, J. Zeng, J. Lumin. 158 (2015) 301.
[16] Z. Zhang, A. Song, S. Song, J. Zhang, W. Zhang, D. Wang, J. Alloys Compd. 629 (2015) 32.
[17] P. Roux, D. Lowor, G. Bonel, CR Acad. Paris: Ser. C 286 (1978) 549.
[18] M. Yashima, A. Sakai, T. Kamiyama, A. Hoshikawa, J. Solid State Chem. 175 (2003) 272.
[19] K. Sugiyama, M. Tokonami, Phys. Chem. Miner. 15 (1987) 125.
[20] S. Zhai, W. Xue, D. Yamazaki, F. Ma, Sci. China Earth Sci. 57 (2014) 2292.
[21] G. Blasse, J. Alloys Compd. 192 (1993) 17.
[22] Y. Liu, B. Lei, C. Shi, Chem. Mater. 17 (2005) 2108.
[23] Z. Yuan, C. Chang, D. Mao, W. Ying, J. Alloys Compd. 377 (2004) 268.

[1] For interpretation of color in Fig. 7, the reader is referred to the web version of this article.

[24] K. Pavani, J. Suresh Kumar, L. Rama Moorthy, Mater. Res. Exp. 1 (2014) 016201.
[25] W. Xue, S. Zhai, H. Zheng, Mater. Chem. Phys. 133 (2012) 324.
[26] J. Mu, L. Liu, S.Z. Kang, Nanoscale Res. Lett. 2 (2007) 100.
[27] S. Yan, J. Mater. Sci. – Mater. Electron. 25 (2014) 1868.
[28] Z. Zhang, Y. Wu, X. Shen, Y. Ren, W. Zhang, D. Wang, Opt. Laser Technol. 62 (2014) 63.
[29] S. Zhai, M. Akaogi, H. Kojitani, W. Xue, E. Ito, Phys. Earth Planet. Inter. 228 (2014) 144.
[30] R.M. Thompson, X. Xie, S. Zhai, R.T. Downs, H. Yang, Am. Mineral. 98 (2013) 1585.
[31] D.A. Grisafe, F.A. Hummel, Am. Mineral. 55 (1970) 1131.
[32] N. Chen, Y. Pan, J.A. Weil, M.J. Nilges, Am. Mineral. 87 (2002) 47.
[33] C. Wu, B. Lin, M. Jean, J. Electron. Mater. 43 (2014) 465.
[34] G. Blasse, Phy. Lett. A 28 (1968) 444.